Eur Radiol (2015) 25:488–496
DOI 10.1007/s00330-014-3427-z

COMPUTED TOMOGRAPHY

Detection and quantification of the solid component in pulmonary subsolid nodules by semiautomatic segmentation

Ernst Th. Scholten · Colin Jacobs · Bram van Ginneken · Sarah van Riel · Rozemarijn Vliegenthart · Matthijs Oudkerk · Harry J. de Koning · Nanda Horeweg · Mathias Prokop · Hester A. Gietema · Willem P. Th.M. Mali · Pim A. de Jong

Received: 12 January 2014 / Revised: 30 August 2014 / Accepted: 2 September 2014 / Published online: 7 October 2014

Abstract

Objective To determine whether semiautomatic volumetric software can differentiate part-solid from nonsolid pulmonary nodules and aid quantification of the solid component.

Methods As per reference standard, 115 nodules were differentiated into nonsolid and part-solid by two radiologists; disagreements were adjudicated by a third radiologist. The diameters of solid components were measured manually. Semiautomatic volumetric measurements were used to identify and quantify a possible solid component, using different Hounsfield unit (HU) thresholds. The measurements were compared with the reference standard and manual measurements.

Results The reference standard detected a solid component in 86 nodules. Diagnosis of a solid component by semiautomatic software depended on the threshold chosen. A threshold of −300 HU resulted in the detection of a solid component in 75 nodules with good sensitivity (90 %) and specificity (88 %). At a threshold of −130 HU, semiautomatic measurements of the diameter of the solid component (mean 2.4 mm, SD 2.7 mm) were comparable to manual measurements at the mediastinal window setting (mean 2.3 mm, SD 2.5 mm [p= 0.63]).

Conclusion Semiautomatic segmentation of subsolid nodules could diagnose part-solid nodules and quantify the solid component similar to human observers. Performance depends on the attenuation segmentation thresholds. This method may prove useful in managing subsolid nodules.

Key Points

- *Semiautomatic segmentation can accurately differentiate nonsolid from part-solid pulmonary nodules*

Trial Registration Dutch-Belgian lung cancer screening trial (NELSON; ISRCTN63545820).
http://www.controlled-trials.com/ISRCTN63545820

E. T. Scholten · H. A. Gietema · W. P. T. Mali · P. A. de Jong (✉)
Department of Radiology, University Medical Center, Heidelberglaan 100, 3584 CX Utrecht, The Netherlands
e-mail: P.deJong-8@umcutrecht.nl

E. T. Scholten
Department of Radiology, Kennemer Gasthuis, Haarlem, The Netherlands

C. Jacobs · B. van Ginneken · S. van Riel
Diagnostic Image Analysis Group, Radboud University Medical Center, Nijmegen, The Netherlands

B. van Ginneken
Fraunhofer MEVIS, Bremen, Germany

R. Vliegenthart
Department of Radiology, University of Groningen, University Medical Center Groningen, Groningen, The Netherlands

R. Vliegenthart · M. Oudkerk
Center for Medical Imaging-North East Netherlands, University of Groningen, University Medical Centre Groningen, Groningen, The Netherlands

H. J. de Koning · N. Horeweg
Department of Public Health, Erasmus Medical Center, Rotterdam, The Netherlands

N. Horeweg
Department of Pulmonology, Erasmus Medical Center, Rotterdam, The Netherlands

M. Prokop
Department of Radiology, Radboud University Medical Center, Nijmegen, The Netherlands

- *Semiautomatic segmentation can quantify the solid component similar to manual measurements*
- *Semiautomatic segmentation may aid management of subsolid nodules following Fleischner Society recommendations*
- *Performance for the segmentation of subsolid nodules depends on the chosen attenuation thresholds*

Keywords Subsolid pulmonary nodules · Computer-aided diagnosis · Computed tomography · Lung cancer · Screening

Introduction

Lung cancer screening with computed tomography (CT) has increased the awareness of a specific subtype of pulmonary nodules—the subsolid nodule (SSN). SSNs can be subdivided into pure nonsolid nodules and part-solid nodules. A non-solid nodule consists only of ground glass, which is defined as increased lung attenuation with preservation of the bronchial and vascular margins. In a part-solid nodule, the solid part of the nodule completely obscures the underlying lung parenchyma. Persistent SSNs have a high likelihood of malignancy, with reported malignancy rates ranging from 19 to 79 % [1, 2].

Precise assessment of the change in diameter of pulmonary nodules on follow-up CT is essential for the evaluation of nodules in lung cancer screening and routine care. For the evaluation of solid pulmonary nodules three-dimensional volumetric assessment has been shown to be more accurate than two-dimensional measurements [3–5].

SSNs are less dense and less well circumscribed than solid nodules and thus more difficult to measure accurately manually or by semiautomatic volumetry. For SSNs, mass has been reported to be a more sensitive parameter to detect progression than volume [6]. Mass, being the product of volume and physical density of the nodule, has the advantage that progression of the nodule will not only depend on an increase in volume, but also progression of a solid component or the appearance thereof will be reflected in this parameter.

In 2013, the Fleischner Society published recommendations for the management of SSNs [7]. It is recommended to measure the diameter of the solid components and to determine the percentage of solid versus ground-glass components of SSNs. This is important because it has been shown that the greater the extent of the solid component, the more likely the lesion will be an invasive adenocarcinoma with an associated poorer prognosis [8–15]. An SSN with a solid component larger than 5 mm should be considered malignant until proven otherwise, and important decisions to possibly resect a nodule are based on this cut-off. This makes an accurate and reproducible method to assess the diameter of the solid component mandatory.

The percentage of ground-glass component of the part-solid SSN can be calculated or determined in different ways. Some calculations are based on the diameter of the different components, and others on the size of the area. Furthermore, different values for the window level and width are used. Aoki et al. used electronic calipers to measure the dimensions of the SSN and the solid component on a lung window [8]. The ground glass opacity (GGO) ratio of the SSN is then based on the dimension of the diameter of the solid part divided by the diameter of the whole nodule (Fig. 1). Other papers report the calculation of the percentage of ground glass area based on the difference of the area total nodule on lung window minus the area the solid component on the mediastinal window with a mean of 40 and a window of 400. This is referred to as the vanishing ratio method [15] or the tumour disappearance rate (TDR) [11, 12], although the ground glass component does not disappear, it becomes invisible on mediastinal windows. This principle has been adopted by the Fleischner Society. In their recommendations [7] it is stated that the solid component should be evaluated with a mediastinal window and the nodule including the ground-glass component should be measured with a lung window when electronic calipers are used.

In previous studies (Scholten et al., 2014, Subsolid pulmonary nodules detected during lung cancer screening: towards a close follow-up approach?, submitted in European Respiratory Journal and [16]) we measured diameter, volume and mass of SSNs with dedicated volumetric software [17]. The aim of the present study was to determine whether this software could differentiate part-solid from nonsolid nodules and quantify the diameter of the solid component at least similar to human observers performing manual measurements.

Material and methods

Subjects

This study is part of the Dutch-Belgian multi-centre randomized low-dose CT lung cancer screening (NELSON) trial. The Minister of Health of the Netherlands and the ethics committees of the participating hospitals approved the NELSON study (number, ISRCTN63545820). Written informed consent was obtained from all participants. For the present study, we included the last CT from all participants with one or more SSNs (total number 115) from the Dutch centres (University Medical Center Groningen, University Medical Center Utrecht and Kennemer Gasthuis, Haarlem, the Netherlands).

CT imaging protocol

CT screening was performed at baseline and 1,3.5 and 5.5 years after baseline plus additional follow-up CT

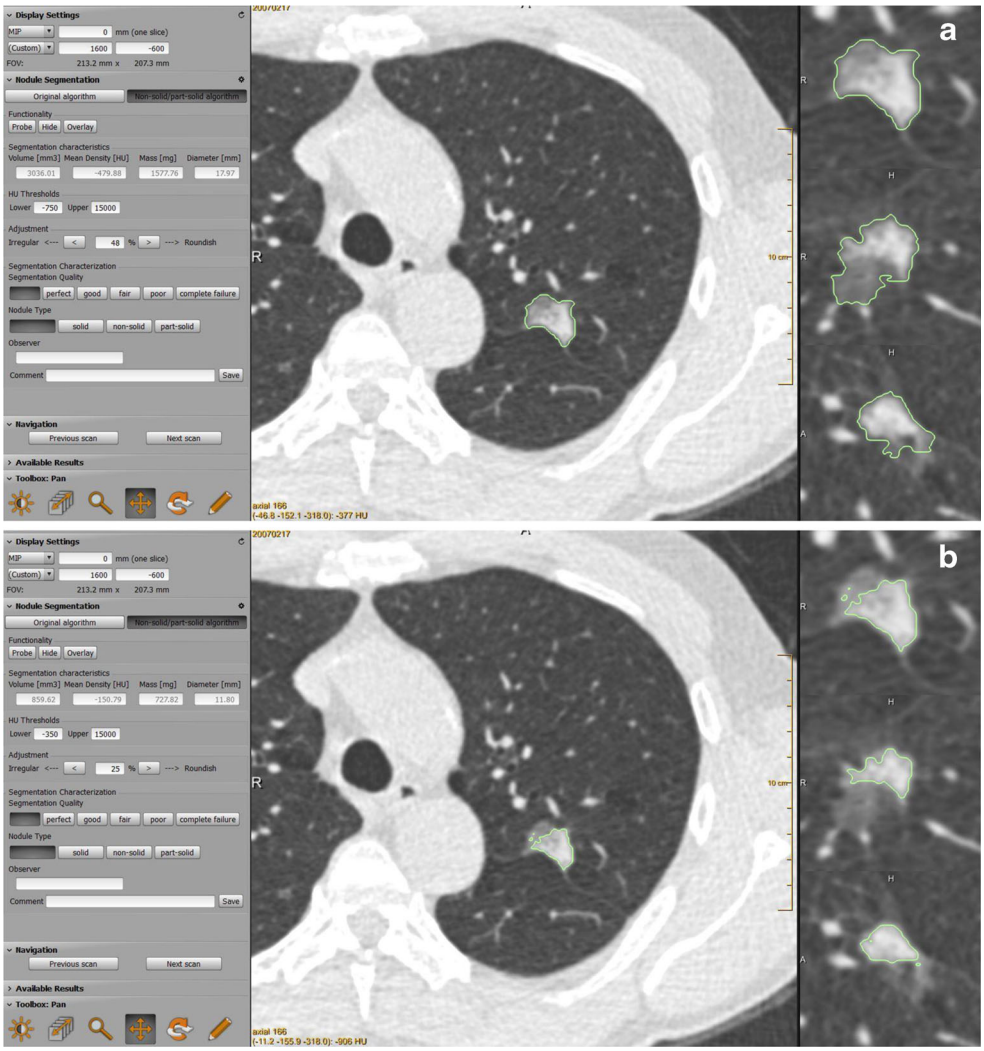

Fig. 1 SSN with a diameter of 18 mm (**a**) and a solid component diameter on lung window of 12 mm (**b**). GGO ratio is (Diameter SSN−Diameter SC)/Diameter SSN)×100=(18−12)/18×100=33.3 %

examinations in case indeterminate nodules were detected [18]. Multidetector-row systems (Somatom Sensation 16, Siemens Medical Solutions, Mx8000 IDT or Brilliance-16, Philips Medical Systems, Cleveland, OH) were used with 16×0.75 mm collimation and pitch 1.3. Unenhanced full inspiration CTs were acquired with 30 mAs at 120 kVp for patients weighing less than 80 kg, and with 30 mAs at 140 kVp for those weighing more. Axial 1.0-mm images were reconstructed at 0.7-mm increment with a 512×512 matrix, using a moderately soft kernel and the smallest field of view that included both lungs. In the trial, CTs were read for SSNs.

Observer protocol

Reference standard for nonsolid and part-solid pulmonary nodules

Two radiologists with more than 10 years' experience with SSNs were asked independently if the nodule was, in their opinion, either nonsolid or part-solid. In case of disagreement, a third chest radiologist with more than 10 years' experience with SSNs decided on the nature of the nodule. This resulted in a human reference standard for all nodules. Interobserver agreement for the presence of a solid component was calculated for the two observers.

Semiautomatic segmentation of the solid component of part-solid nodules

We previously measured diameter, volume and mass for the 115 SSNs (CIRRUS Lung, Diagnostic Image Analysis Group, Nijmegen, the Netherlands, Fraunhofer MEVIS, Bremen, Germany). This prototype software program has been described previously [17] and was adapted to handle SSNs. The user can either click a centre point or draw a stroke on the largest diameter of the nodule as an input to the algorithm. Based on this user input, a volume of interest (VOI) is automatically defined around the nodule. An initial segmentation is acquired by region growing using thresholds applicable to subsolid nodules. The default value for the lower threshold is

−750 HU, and for the higher threshold −150 HU. If the segmentation is found to be acceptable the result can be stored after this single input. Two parameters, density threshold value and roundness versus irregularity, can be adjusted by the user of the program to optimize the segmentation if this is felt to be necessary by the observer. This requires an extra mouse click for every adaption of the segmentation until the result is acceptable to the observer.

Finally, a sequence of morphological operations is used to remove the chest wall and adjacent vessels, if applicable.

For the present study, we added segmentation of the solid component. To determine the most suitable segmentation threshold we used seven different lower thresholds ranging from −500 to −200 HU, increasing the lower threshold in steps of 50 HU. The upper threshold was fixed at 15,000 HU.

A mediastinal window with a mean of 40 and a window width of 400 implies that only the part of the SSN with densities higher than −160 HU will be visible in the image. So additionally, we performed the segmentations using an eighth lower threshold of −160 HU in order to compare our segmentation with the manual measurements to a mediastinal setting as recommended by the Fleischner recommendations. On the basis on the results of these eight segmentations, we decided to perform an extra ninth segmentation with a lower threshold of −130 HU. The centre of the nodule was preset on the basis of the previous segmentation of the whole SSN. The images show a zoomed nodule in cross-section with the three zoomed in axial (top), coronal (middle) and sagittal (bottom) planes next to it, respectively (Fig. 1). The observer could scroll through the images in all three planes. The segmentation of the solid component was indicated by a continuous line.

For the semiautomatic measurements an apparent solid component of any dimension was considered positive and thus indicative of a part-solid SSN. Measurements in which the software could not segment any solid area were considered negative and indicative of a nonsolid SSN.

Statistical analysis

Data are presented as mean and standard deviation (SD) or median and interquartile range (IQR). Observer agreement for the manual measurements on the mediastinal and lung window was calculated using an intraclass correlation coefficient and for a nonsolid versus part-solid as Cohen kappa. A paired Student *t* test was used for the difference between the semiautomatic segmentation of the solid component and the average of the two manual measurements, and a Fisher's exact test for the difference in the detection of a solid component greater than 5 mm. A Pearson correlation coefficient was used to study the relation between the lower threshold and the measured diameter of the solid component. Sensitivity, specificity, positive predictive value (PPV) and negative predictive value (NPV) were calculated for the presence of a solid component for the eight semiautomatic segmentations and for the manual measurements.

A McNemar's test and the area under the curve (AUC) from the ROC analysis were performed.

P values less than 0.05 were considered significant. Statistical analysis was performed with software (IBM SPSS version 20, SPSS, Chicago).

Results

Visual SSN evaluation

In 78 out of the 115 cases (67.8 %) both observers agreed on the part-solid and in 23 cases (20.0 %) on the nonsolid character of the SSN. In 14 cases (12.1 %) they disagreed, in six cases only observer 1 considered the SSN to be part-solid, in eight cases only observer 2. Those 14 cases were adjudicated by the third reader to part-solid ($n=8$) or nonsolid ($n=6$). After this third reading 86 SSNs were labelled part-solid and 29 nonsolid. Observer agreement was good with a Cohen kappa value of 0.68 (Table 1).

Semiautomatic segmentation of the solid component

In three cases of bubbly SSNs, a single solid component could not be indentified and segmented. In five more cases, a vessel running through the SSN precluded a good segmentation of the solid component. These eight cases were excluded, resulting in 107 cases available for further evaluation: 83 (77.6 %) part-solid and 24 (22.4 %) nonsolid nodules. In nine cases the segmentation had to be adjusted in one or more thresholds by replacing the seed point because a vessel was partly segmented.

Detection of the solid component

Sensitivity and specificity of detecting the solid component was dependent on the threshold chosen (Table 2; Fig. 2a, b). Sensitivity/specificity ranged from 99 %/42 % for −500 HU to 65%/88% for −160 HU, respectively. A low threshold of

Table 1 Visual evaluation of character of 115 SSNs

		Observer 1		Total
		Part-solid	Nonsolid	
Observer 2	Part-solid	78	8	86
	Non solid	6	23	29
Total		84	31	115

Table 2 Detection of the solid component with semiautomatic segmentation with different lower thresholds and with manual measurement with a mediastinal window of 40/400 for comparison

	TP	FP	FN	TN	Sens	Spec	PPV	NPV	Tot.
−500 HU	82	14	1	10	99 %	42 %	85 %	91 %	107
−450 HU	80	8	3	16	96 %	67 %	91 %	84 %	107
−400 HU	78	7	5	17	94 %	71 %	92 %	77 %	107
−350 HU	76	4	7	20	92 %	83 %	95 %	74 %	107
−300 HU	75	3	8	21	90 %	88 %	96 %	72 %	107
−250 HU	70	3	13	21	84 %	88 %	96 %	62 %	107
−200 HU	64	3	19	21	77 %	88 %	96 %	53 %	107
−160 HU	54	4	29	20	65 %	88 %	93 %	41 %	107
Manual	51	1	32	23	61 %	96 %	98 %	42 %	107

TP true positive, *FP* false positive, *FN* false negative, *TN* true negative, *Sens* sensitivity, *Spec* specificity, *PPV* positive predictive value, *NPV* negative predictive value

−500 HU resulted in a high sensitivity at the cost of a low specificity. Increasing the lower threshold to −200 HU increased the specificity to near 90 % while the sensitivity dropped to 77 %. A threshold of −300 HU resulted in a sensitivity of 90 % a specificity of 88 % with a PPV of 96 % and an NPV of 72 %. The AUC for this threshold was maximal 0.889. This was not significantly different from the AUC values of −350 HU, −400 HU and −500 HU with *p* values of 0.4947, 0.1045 and 0.0949 respectively (Table 3).

Diameter of the solid component with various thresholds

The mean diameter of the apparent solid component depended on the threshold and the diameters varied by about a factor 3 in the first eight segmentations from 2.7 mm (SD 2.76 mm) at −160 HU to 7.3 mm (SD 3.83 mm) at −500 HU (Table 4). The relationship between threshold and diameter of the solid component was nearly linear (Pearson correlation −0.99, Fig. 3).

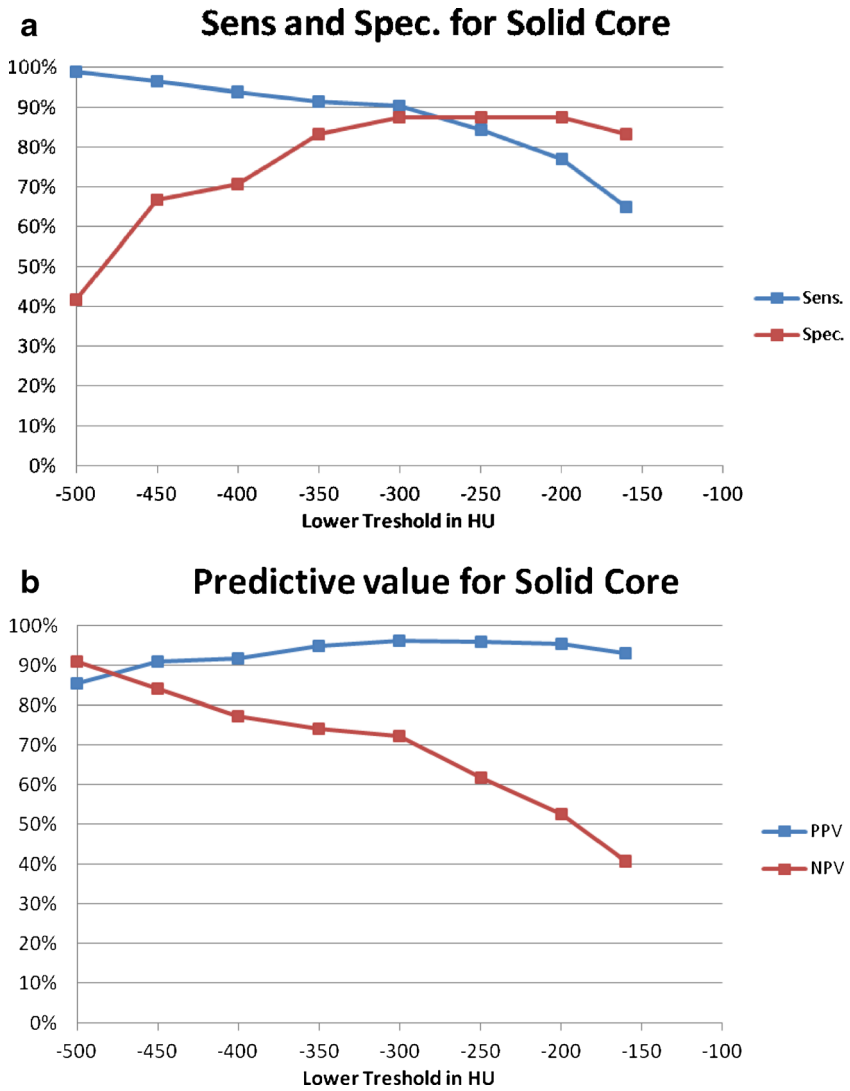

Fig. 2 Sensitivity and specificity (**a**) and positive predictive value and negative predictive value (**b**) for the detection of the solid component with semiautomatic segmentation as a function of the lower density threshold

Table 3 DeLong's test for two correlated ROC curves

Cut-off	AUC	AUC *P* value	McNemar *P* value sens	McNemar *P* value spec
−500 HU	0.702	0.0006	0.0082	0.0009
−450 HU	0.815	0.0949	0.0253	0.0253
−400 HU	0.824	0.1045	0.0833	0.0455
−350 HU	0.874	0.4947	0.317	0.317
−300 HU	0.889	Reference	Reference	Reference
−250 HU	0.859	0.02187	0.0253	NA
−200 HU	0.823	0.0004	0.0009	NA
−160 HU	0.763	<0.0001	<0.0001	NA

The threshold of −300 HU was taken as reference for the test of significance

Comparison of manual and semiautomatic solid component measurement

Manual measurement of the solid component with a lung window setting resulted in a mean diameter of the solid component of 5.1 mm (SD 2.4 mm) for observer 1 and 3.8 mm (SD 2.0 mm) for observer 2; agreement between observers was good with an intraclass correlation coefficient of 0.706. Mean measurement for the two observers was 4.4 mm (SD 2.0 mm).

Manual measurement of the solid component with a mediastinal window (40/400 HU) resulted in a mean diameter of 2.4 mm (SD 2.6 mm) for observer 1 and 2.2 mm (SD 2.8 mm) for observer 2. Agreement between observers was good with intraclass correlation coefficients of 0.781. Mean measurement of the two observers was 2.3 mm (SD 2.5 mm). This was significantly smaller (17 %) than the semiautomatic measurements at −160 HU with a mean diameter of 2.7 mm (SD 2.8 mm) (p=0.03). Because of this significant difference we decided to add an extra, ninth segmentation with the sole purpose of investigating whether we could decrease this difference to almost zero. On the basis of this linear relationship between the lower threshold and the measured diameter of the solid core we calculated that a segmentation with a lower threshold of −130 HU would result in a mean diameter of the solid component of 2.29 mm. This ninth segmentation actually resulted in a mean diameter of 2.40 mm (SD 2.67 mm). This was not significantly different from the manual measurements (p=0.63).

Table 4 Size of the apparent solid component in the part-solid SSNs with semiautomatic segmentation and with manual measurements with mediastinal and lung window

Threshold (HU)	Mean size solid component (mm)	SD
−500	7.3	3.8
−450	6.6	3.8
−400	5.9	3.5
−350	5.2	3.4
−300	4.7	3.3
−250	3.8	3.1
−200	3.2	3.0
−160	2.7	2.8
−130	2.4	2.7
Manual		
Mediastinal window	2.3	2.5
Lung window	4.4	2.0

Manual measurement with mediastinal window is equivalent to semiautomatic measurement with a lower threshold of −130 HU. Manual measurement with lung window turns out to be best comparable with semiautomatic measurement with a lower threshold of −300 HU

The automatic segmentations with a lower threshold of −160 HU resulted in 18, and with a lower threshold of −130 HU resulted in 15 lesions with a solid component larger than 5 mm while manual measurements resulted in only 13 lesions with a solid component larger than 5 mm. The difference between the automatic segmentations and the manual measurements was not significant (p=0.29 and 0.41, respectively).

Discussion

Our study focused on the role of semiautomatic segmentation in the implementation of the Fleischner Society recommendations for SSN management. Volumetry of solid pulmonary nodules has been shown to be more accurate and reproducible than two-dimensional measurements [5]. As it is conceivable that automated analysis reduces observer variation, semiautomatic segmentation may prove useful for the diagnosis of solid components and measurement of growth of SSNs. We showed that semiautomatic segmentation can detect a solid component and thus diagnose the part-solid nature of an SSN with a good accuracy. We think that a lower threshold of −300 HU with a sensitivity of 90 % and a specificity of 88 % is a good compromise between the number of false positives and false negatives. However the exact choice of the threshold will depend on the emphasis that an individual screening program wants to place in the trade-off between optimization of specificity or sensitivity. Furthermore, semiautomatic segmentation was able to measure the diameter of the solid component similar to manual measurements. Consequently it can differentiate between solid components larger or smaller than 5 mm. This diameter is considered critical by the Fleischner Society. According to their recommendations, a persistent or growing solid component greater than 5 mm should be considered malignant until proven otherwise. Therefore, the semiautomatic software can help to distinguish nodules that should be resected from those that can be

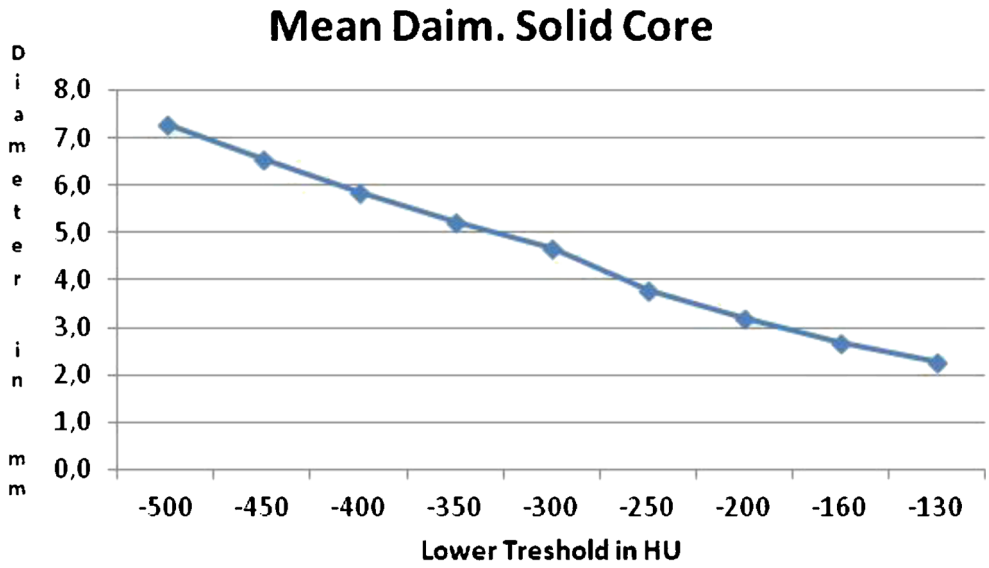

Fig. 3 Mean size of the apparent solid component in the part-solid SSNs with semiautomatic segmentation

followed, but thresholds are of crucial importance. When using a lower threshold of −160 HU (mediastinal setting) as proposed by the Fleischner Society the measurement of the diameter of the solid component increases by on average 17 % when compared to manual measurements with a mediastinal window of 40/400.

When the lower threshold is increased to −130 HU, the difference with manual measurements is reduced and is no longer significant. In the absence of a proper reference standard these cut-offs are arbitrary, but with our software −130 HU corresponds favourably to the Fleischner recommendations.

Provided a lower threshold of the segmentation of −300 HU is chosen for the measurement of the diameter of the solid component, the results are comparable with manual measurements at a lung window. Hence, the described methodology, if replicated, may prove useful in the diagnosis and follow-up of SSNs.

Numerous papers relate quantitative or semiquantitative data of SSNs to the clinical outcome in various ingenious ways. But as stated in the Fleischner recommendations [7] no consensus regarding an optimal approach has been sufficiently validated. Kakinuma et al. [15] evaluated four measuring methods for SSNs for the prediction of the clinical outcome of patients with a peripheral non-small cell lung cancer. They concluded that the vanishing ratio was the most useful predictor of the outcome. This vanishing ratio reflects the part of the tumour that disappears on the image with a mediastinal setting as compared to the image with a lung window. The same principle is applied in the tumour disappearance rate (TDR) as introduced by Takamochi et al. [11] and applied by Okada et al. [12]. They distinguished four groups of TDR: less than 25 %, between 25 and 50 %, between 50 and 75 %, and more than 75 % in their series of 127 peripheral adenocarcinomas of the lung. They concluded that their findings correlated well with histological prognostic factors. Since the TDR was over 75 % in 98 % of our cases of part-solid SSNs, this ratio was not useful to make any further differentiation in our series. The discrepancy between our results and those of Okade is probably due to the fact that we studied small SSNs, mainly part-solid nodules with a relatively small solid component.

Several other papers report on attempts for objective methods other than the calculation of GGO ratio and TDR to evaluate the quantitative aspects and characterization of an SSN [19–24]. Some use a one-dimensional analysis [22, 24] by measuring the diameter or a combination of diameter and density of the components of an SSN on a one-dimensional histogram of the nodule. Yanagawa et al. [22] in a study of 96 adenocarcinomas concluded that for the ratio of solid component to total tumour, using the profile curves is more useful in estimating prognostic factors than visual assessment. Kitami et al. [23] concluded that a mean CT density value measured on a line through the maximum diameter of the nodule is useful to select between "follow-up or resection" strategies, and that lesions smaller than 1 cm and a mean CT density lower than −600 HU are pre-invasive. The analysis of the attenuation coefficients in a three-dimensional histogram of the SSN is another approach to differentiate premalignant from malignant SSNs (Scholten et al., 2014, Subsolid pulmonary nodules detected during lung cancer screening: towards a close follow-up approach?, submitted in European Respiratory Journal). Ikeda et al. concluded in their study that two peaks on the CT number histogram can rule out atypical adenomatous hyperplasia and that the analysis of the CT density numbers can be used to differentiate between atypical adenomatous hyperplasia and bronchoalveolar cell carcinoma and between bronchoalveolar cell carcinoma and adenocarcinoma. Maldonado et al. [24] included features of the texture of the nodule in their analysis for risk stratification of nodules of

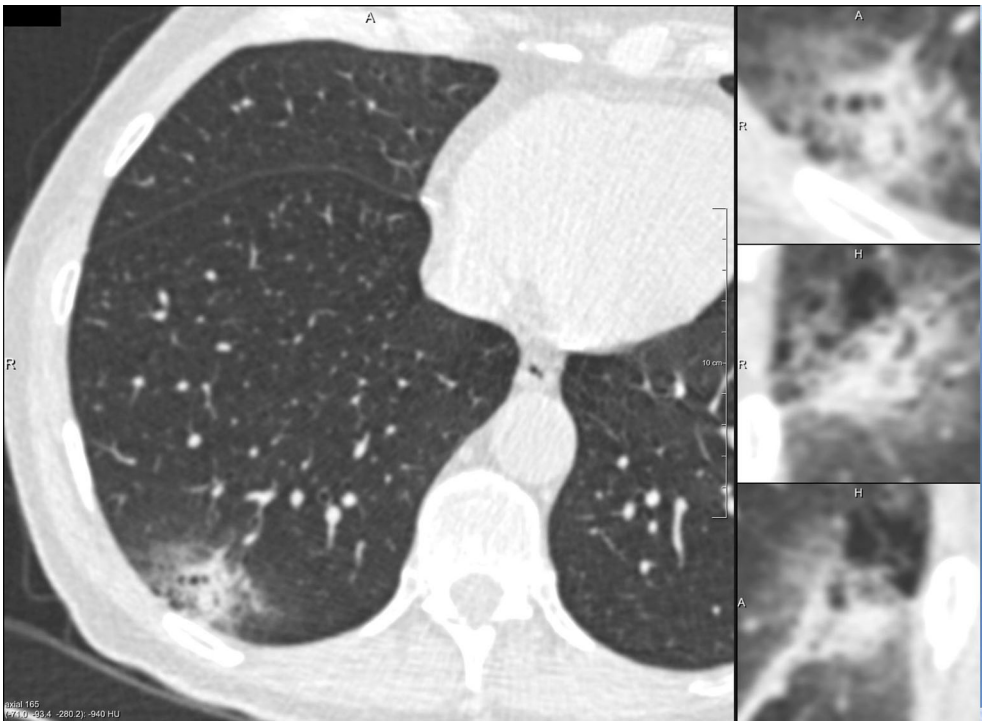

Fig. 4 Bubbly lesions in which the system failed to calculated the mass of the solid parts. These cases had to be excluded

the lung adenocarcinoma spectrum. Clearly a head-to-head comparison of all these methods is beyond the scope of our article. However, when a nodule is segmented successfully, our method is straightforward and intuitive and enables both diagnosis and measurement of all crucial nodule aspects as proposed in the Fleischner recommendations.

Our study has several limitations. First, the software sometimes includes parts of a vessel passing through the SSN in the segmentation, which resulted in an apparent solid component in five SSNs that were considered nonsolid by two observers. These cases had to be excluded. In a further nine cases, the segmentation of the solid component had to be adjusted since part of a vessel was included in the segmentation. From this finding we concluded that visual inspection of the result of the semiautomatic segmentation remains necessary until this technical challenge is solved. Nevertheless, as a sufficient number of nodules remained in our analysis, we think that this limitation does not invalidate our results. Second, the system failed to segment the solid parts in three bubbly lesions, so these cases had to be excluded too (Fig. 4). Third, we have no histological confirmation of the nature of our nodules so we were not able to make a subgroup analysis of groups with different histology and we have no proof of the nonsolid or part-solid aspect of the lesions, nor of the diameter of the solid component. Nevertheless we used three human experts to decide on the aspect of the nodule and compared semiautomatic measurements with manual measurements that are currently used.

Fourth, our results are valid only for a set of nodules that was predominantly ground-glass, and have not been tested on a sample of part-solid nodules with varying proportions of a solid component.

Finally, our results are valid only for the software we used and our thresholds need replication in an independent cohort.

In conclusion, we have shown that semiautomatic segmentation of SSNs can differentiate between nonsolid and part-solid lesions with good sensitivity and specificity provided that no vessel segments are included in the segmentation. Furthermore the diameter of the solid component of a part-solid SSN as defined by the recommendations of the Fleischner Society can be measured semiautomatically with results comparable to the manual measurements.

In combination with the diameter of the complete SSN this can be used to calculate the GGO ratio.

Acknowledgments The scientific guarantor of this publication is Prof. W.P.Th.M. Mali. The authors of this manuscript declare no relationships with any companies whose products or services may be related to the subject matter of the article. The NELSON study has received funding by Zorg Onderzoek Nederland-Medische Wetenschappen (ZonMw), KWF Kankerbestrijding, Stichting Centraal Fonds Reserves van Voormalig Vrijwillige Ziekenfondsverzekeringen (RvvZ), G. Ph. Verhagen Foundation, Rotterdam Oncologic Thoracic Study Group (ROTS) and Erasmus Trust Fund, Stichting tegen Kanker, Vlaamse Liga tegen Kanker and LOGO Leuven and Hageland. One of the authors has significant statistical expertise and no complex statistical methods were necessary for this paper. Institutional review board approval was obtained. Written informed consent was obtained from all subjects (patients) in this study. Methodology: retrospective, observational, multicentre study.

References

1. Henschke CI, Yankelevitz DF, Mirtcheva R, McGuinness G, McCauley D, Miettinen OS (2002) CT screening for lung cancer: frequency and significance of part-solid and nonsolid nodules. AJR Am J Roentgenol 178:1053–1057
2. Sone S, Nakayama T, Honda T et al (2007) Long-term follow-up study of a population-based 1996-1998 mass screening programme for lung cancer using mobile low-dose spiral computed tomography. Lung Cancer 58:329–341
3. Revel MP, Lefort C, Bissery A et al (2004) Pulmonary nodules: preliminary experience with three-dimensional evaluation. Radiology 231:459–466
4. Revel MP, Bissery A, Bienvenu M, Aycard L, Lefort C, Frija G (2004) Are two-dimensional CT measurements of small noncalcified pulmonary nodules reliable. Radiology 231:453–458
5. Marten K, Auer F, Schmidt S, Kohl G, Rummeny EJ, Engelke C (2006) Inadequacy of manual measurements compared to automated CT volumetry in assessment of treatment response of pulmonary metastases using RECIST criteria. Eur Radiol 16:781–790
6. de Hoop B, Gietema H, van de Vorst S, Murphy K, van Klaveren RJ, Prokop M (2010) Pulmonary ground-glass nodules: increase in mass as an early indicator of growth. Radiology 255:199–206
7. Naidich DP, Bankier AA, MacMahon H et al (2013) Recommendations for the management of subsolid pulmonary nodules detected at CT: a statement from the Fleischner Society. Radiology 266:304–317
8. Aoki T, Tomoda Y, Watanabe H et al (2001) Peripheral lung adenocarcinoma: correlation of thin-section CT findings with histologic prognostic factors and survival. Radiology 220:803
9. Kim EA, Johkoh T, Lee KS et al (2001) Quantification of ground-glass opacity on high-resolution CT of small peripheral adenocarcinoma of the lung: pathologic and prognostic implications. AJR Am J Roentgenol 177:1417–1422
10. Ohde Y, Nagai K, Yoshida J et al (2003) The proportion of consolidation to ground-glass opacity on high resolution CT is a good predictor for distinguishing the population of non-invasive peripheral adenocarcinoma. Lung Cancer 42:303–310
11. Takamochi K, Nagai K, Yoshida J et al (2001) Pathologic N0 status in pulmonary adenocarcinoma is predictable by combining serum carcinoembryonic antigen level and computed tomographic findings. J Thorac Cardiovasc Surg 122:325–330
12. Okada M, Nishio W, Sakamoto T, Uchino K, Tsubota N (2003) Discrepancy of computed tomographic image between lung and mediastinal windows as a prognostic implication in small lung adenocarcinoma. Ann Thorac Surg 76:1828–1832
13. Yanagawa M, Tanaka Y, Kusumoto M et al (2010) Automated assessment of malignant degree of small peripheral adenocarcinomas using volumetric CT data: correlation with pathologic prognostic factors. Lung Cancer 70:286–294
14. Sumikawa H, Johkoh T, Nagareda T et al (2008) Pulmonary adenocarcinomas with ground-glass attenuation on thin-section CT: quantification by three-dimensional image analyzing method. Eur J Radiol 65:104–111
15. Kakinuma R, Kodama K, Yamada K et al (2008) Performance evaluation of 4 measuring methods of ground-glass opacities for predicting the 5-year relapse-free survival of patients with peripheral nonsmall cell lung cancer: a multicenter study. J Comput Assist Tomogr 32:792–798
16. Scholten ET, Jacobs C, van Ginneken B et al (2013) Computer aided segmentation and volumetry of artificial ground glass nodules on chest computed tomography. AJR Am J Roentgenol 201:295–300
17. Kuhnigk JM, Dicken V, Bornemann L et al (2006) Morphological segmentation and partial volume analysis for volumetry of solid pulmonary lesions in thoracic CT scans. IEEE Trans Med Imaging 25:417–434
18. van Klaveren RJ, Oudkerk M, Prokop M et al (2009) Management of lung nodules detected by volume CT scanning. N Engl J Med 361: 2221–2229
19. Bhure UN, Lardinois D, Kalff V et al (2010) Accuracy of CT parameters for assessment of tumour size and aggressiveness in lung adenocarcinoma with bronchoalveolar elements. Br J Radiol 83:841–849
20. Nakata M, Sawada S, Yamashita M et al (2005) Objective radiologic analysis of groundglass opacity aimed at curative limited resection for small peripheral non–small cell lung cancer. J Thorac Cardiovasc Surg 129:1226–1231
21. Ikeda K, Awai K, Mori T, Kawanaka K, Yamashita Y, Nomori H (2007) Differential diagnosis of ground-glass opacity nodules: CT number analysis by three-dimensional computerized quantification. Chest 132:984–990
22. Yanagawa M, Kuriyama K, Kunitomi Y et al (2009) One-dimensional quantitative evaluation of peripheral lung adenocarcinoma with or without ground-glass opacity on thin-section CT images using profile curves. Br J Radiol 82:532–540
23. Kitami A, Kamio Y, Hayashi S et al (2012) One-dimensional mean computed tomography value evaluation of ground-glass opacity on high-resolution images. Gen Thorac Cardiovasc Surg 60:425–430
24. Maldonado F, Boland JM, Raghunath S (2013) Noninvasive characterization of the histopathologic features of pulmonary nodules of the lung adenocarcinoma spectrum using computer-aided nodule assessment and risk yield (CANARY)–a pilot study. J Thorac Oncol 8:452–460